ISSN 2229-5518

Effect of Nanofluid Concentration on the Performance of Circular Heat Pipe

M. G. Mousa

Abstract— The goal of this paper is to experimentally study the behavior of nanofluid to improve the performance of a circular heat pipe. Pure water and Al_2O_3-water based nanofluid are used as working fluids. An experimental setup is designed and constructed to study the heat pipe performance under different operating conditions. The effect of filling ratio, volume fraction of nano-particle in the base fluid, and heat input rate on the thermal resistance is investigated. Total thermal resistance of the heat pipe for pure water and Al_2O_3-water based nanofluid is also predicted. An experimental correlation is obtained to predict the influence of Prandtl number and dimensionless heat transfer rate, K_q on thermal resistance. Thermal resistance decreases with increasing Al_2O_3-water based nanofluid compared to that of pure water. The experimental data is compared to the available data from previous work. The agreement is found to be fairly good.

Index Terms— Heat Pipe, Thermal Performance, Nanofluids

Nomenclature

A	Surface area, m^2
FR	Filling ratio
I	Electric current, Amp
k	thermal conductivity, W/m.K
N	Number of thermocouples
Q	Input heat rate, W
q	Heat flux, W/m^2
R	Total thermal resistance of heat pipe, K/W
T	Temperature, K
V	Applied voltage, Volt
X	Horizontal coordinate parallel to the test section, mm

Greek Symbols

ϕ	Volume fraction of nanoparticles, %
ρ	Density, kg/m^3
μ	Dynamic viscosity, $N.s/m^2$

Subscript

c	Condenser
e	Evaporator
ef	Effective
e	Evaporator
l	Liquid
m	Base fluid
n	Nanofluid
p	Particles
water	Pure water

Dimensionless Numbers

RR Reduction factor in thermal resistance

K_q Dimensionless heat transfer rate, $\dfrac{K_{ef} \times L_e \times \Delta T}{Q}$

Pr Prandtl number, $\dfrac{\mu_{ef} \times Cp_{ef}}{K_{ef}}$

INTRODUCTION

To solve the growing problem of heat generation by electronic equipment, two-phase change devices such as heat pipe and thermosyohon cooling systems are now used in electronic industry. Heat pipes are passive devices that transport heat from a heat source to a heat sink over relatively long distances via the latent heat of vaporization of a working fluid. The heat pipe generally consists of three sections; evaporator, adiabatic section and condenser. In the evaporator, the working fluid evaporates as it absorbs an amount of heat equivalent to the latent heat of vaporization. The working fluid vapor condenses in the condenser and then, returns back to the evaporator. Nanofluids, produced by suspending nano-particles with average sizes below 100 nm in traditional heat transfer fluids such as water and ethylene glycol provide new working fluids that can be used in heat pipes. A very small amount of guest nano-particles, when uniformly and suspended stably in host fluids, can provide dramatic improvement in working fluid thermal properties. The goal of using nanofluids is to achieve the highest possible thermal properties using the smallest possible volume fraction of the nano-particles (preferably < 1% and with particle size<50 nm) in the host fluid.

Kaya et al. [1] developed a numerical model to simulate the transient performance characteristics of a loop heat pipe. Kang et al. [2], investigated experimentally, the performance of a conventional circular heat pipe provided with deep grooves using nanofluid. The nanofluid used in their study was aqueous solution of 35 nm diameter silver nano-particles. It is reported that, the thermal resistance decreased by 10-80% compared to that of pure water.

Pastukhov et al. [3], experimentally, investigated the performance of a loop heat pipe in which the heat sink was an external air-cooled radiator. The study showed that the use of additional active cooling in combination with loop heat pipe increases the value of dissipated heat up to 180 W and decreases the system thermal resistance down to 0.29 K / W.

Chang et al. [4] investigated, experimentally, the thermal performance of a heat pipe cooling system with thermal resistance model. An experimental investigation of thermosyphon thermal performance considering water and dielectric heat transfer liquids as the working fluids was performed by Jouhara et al. [5]. The copper thermosyphon was 200 mm long with an inner diameter of 6 mm. Each thermosyphon was charged with 1.8 ml of working fluid and tested with an evaporator length of 40 mm and a condenser length of 60 mm. The thermal performance of the water charged thermosyphon is compared with the three other working fluids (FC-84, FC-77 and FC-3283). The parameters considered were the effective thermal resistance as well as the maximum heat transport. These fluids have the advantage of being dielectric which may be better suited for sensitive electronics cooling applications. Furthermore, they provide adequate thermal performance up to approximately 50 W, after which liquid entrainment compromises the thermosyphon performance.

Lips et al. [6], studied experimentally, the performance of plate heat pipe (FPHP). Temperature fields in the heat pipe were measured for different filling ratios, heat fluxes and vapor space thicknesses. Experimental results showed that the liquid distribution in the FPHP and consequently its thermal performance depends strongly on both the filling ratio and the vapor space thickness. A small vapor space thickness induces liquid retention and thus reduces the thermal resistance of the system. Nevertheless, the vapor space thickness influences the level of the meniscus curvature radii in the grooves and hence reduces the maximum capillary pressure. Thus, it must be, carefully, optimized to improve the performance of the FPHP. In all the cases, the optimum filling ratio obtained, was in the range of one to two times the total volume of the grooves. A theoretical approach, in non-working conditions, was developed to model the distribution of the liquid inside the FPHP as a function of the filling ratio and the vapor space thickness.

Das et al. [7-8] and Lee et al. [9]) found great enhancement of thermal conductivity (5-60%) over the volume fraction range of 0.1 to 5%.

All these features indicate the potential of nanofluids in applications involving heat removal. Issues, concerning stability of nanofluids, have to be addressed before they can be put to use. Ironically, nanofluids of oxide particles are more stable but less effective in enhancing thermal conductivity in comparison with nanofluids of metal particles.

The aim of the present work is to investigate, experimentally, the thermal performance of a heat pipe. The affecting parameters on thermal performance of heat pipe are studied. The type of working fluid (pure water and Al_2O_3-water based nanofluid), filling ratio of the working fluid, volume fraction of nano-particles in the base fluid, and heat input rate are considered as experimental parameters. Empirical correlation for heat pipe thermal performance, taking into account the various operating parameters, is presented.

2. Experimental Setup and Procedure

A schematic layout of the experimental test rig is shown in Fig.1. This research adopts pure water and Al_2O_3-water based nanofluid as working fluids. The size of nano-particles is 40 nm. The test nanofluid is obtained by dispersing the nano-particles in pure water. The working fluid is charged through the charging line (6). In the heat pipe, heat is generated using an electric heater (12). The vapor generated in the evaporator section (8) is moved towards the condenser section (4) via an adiabatic tube (5) whose diameter and length are 20 mm and 40 mm, respectively. Both evaporator and condenser sections have the size of 40 mm-diameter and 60 mm-height. The condensate is allowed to return back to evaporator section by capillary action "wick structure" through the adiabatic tube. The surfaces of the evaporator section, adiabatic section, and condenser section sides are covered with 25 mm-thick glass wool insulation (3). Seventeen calibrated cooper-constantan thermocouples (T-type) are glued to the heat pipe surface and distributed along its length to measure the local temperatures (Fig. 2). Two thermocouples are used to

measure ambient temperature. All thermocouples are connected to a digital temperature recorder via a multi-point switch. The non condensable gases are evacuated by a vacuum pump. The heat pipe is evacuated u to 0.01 bar via the vacuum line (10). The power supplied to the electric heater (12) is measured by a multi-meter (13). The input voltage was adjusted, using an autotransformer (2). The voltage drops across the heater were varied from 5 to 45 Volts. The A.C. voltage stabilizer (1) is used to ensure that there is no voltage fluctuation during experiments. The pressure inside the evaporator was measured by a pressure gage with a resolution of 0.01 bar.

Thermocouples (with the uncertainty lower than 0.20 ^{o}C) are distributed along the surfaces of the heat pipe sections as follows: six thermocouples are attached to the evaporator section, two thermocouples are attached to the adiabatic section, and nine thermocouples are attached to the condenser section. The obtained data for temperatures and input heat rate are used to calculate the thermal resistance.

One can define the filling ratio, FR, as the volume of charged fluid to the total evaporator volume. The working fluid is charged at 30 ^{o}C.

The effects of working fluid type, filling ratio, volume fraction of nano-particles in the base fluid, and heat input rate on the thermal performance of the heat pipe are investigated in the experimental work. The experimental runs are executed according to the following steps:

1. The heat pipe is evacuated and charged with a certain amount of working fluid
2. The supplied electrical power is adjusted manually at the desired rate using the autotransformer.
3. The steady state condition is achieved after, approximately, one hour of running time using necessary adjustments to the input heat rate. After reaching the steady state condition, the readings of thermocouples are recorded, sequentially, using the selector switch. The voltage of the heater is measured to determine the value of applied heat flux. Finally, the pressure inside the evaporator is recorded.
4. At the end of each run, power is changed and step 3 is repeated.
5. Steps 1 through 4 are repeated using with another adjusted amount of working fluid. The filling ratios, FR, used are 0.2, 0.4, 0.45, 0.50, 0.55, 0.60, 0.65, 0.70, 0.80 and 1.0.

Pure water and Al_2O_3-water based nanofluid are used as working fluids. Steps 1 through 5 are repeated for Al_2O_3-water based nanofluid using several values of volume fractions of nano-particles. The volume fractions used are 0.25%, 0.4%, 0.5%, 0.6%, 0.75%, 1.0% and 1.5%, respectively.

3. Data Reduction

Although heat pipes are very efficient heat transfer devices, they are subject to a number of heat transfer limitation. For high heat flux heat pipes operating in low to moderate temperature range, the capillary effect and boiling limits are commonly the dominant factor. For a given capillary wick structure and working fluid combination, the pumping ability of the capillary structure to provide the circulation for a given working fluid is limited. In order to maintain the continuity of the interfacial evaporation, capillary pressure must satisfy the following relation [2]

$$\Delta P \geq \Delta P_l + \Delta P_v + P_e + P_c \quad (1)$$

Boiling limit is directly related to bubble formation in the liquid. In order that a bubble can exist and grow in liquid, a certain amount of superheat is required. Accurately characterizing the thermal power transfer, Q is a complicated task because it is difficult to accurately quantify the energy loss to the ambient surroundings. Therefore, the whole surface of the heat pipe is well insulated so that the rate of heat loss can be ignored. The heat input rate can be calculated using the supplied voltage and measured current such that,

$$Q = I \times V \quad (2)$$

Where V and I are the applied voltage in Volt and current in Amp, respectively.

The experimental determination of the thermal performance of the heat pipe requires accurate measurements of evaporator and condenser surface temperatures as well as the power transferred. Calculating evaporator and condenser temperatures is, relatively, a straightforward task. They are obtained by simply averaging the temperature measurements along the evaporator and condenser surfaces. Thus, evaporator and condenser temperatures can be expressed as:

$$\overline{T}_e = \frac{\sum_{i=1}^{i=N_{te}} T_{e\,i}}{N_e}, \quad \overline{T}_c = \frac{\sum_{i=1}^{i=N_{tc}} T_{c_i}}{N_c} \quad (3)$$

Where; N_e, N_c are the number of thermocouples on the evaporator and condenser, respectively. The obtained data for temperatures and heat input rate are then used to calculate the thermal resistance using the following relation,

$$R = \frac{(\overline{T}_e - \overline{T}_c)}{Q} \quad (4)$$

One can assume that the nano-particles are well dispersed within the base-fluid, so the effective physical properties are described by classical formulas which are mentioned by Das et al. [10] as;

$$\rho_{ef} = (1-\phi)\rho_m + \phi \rho_p$$

The effective dynamic viscosity of nanofluids can be calculated using different existing equations that have been obtained for two-phase mixtures. The following relation is the well-known Einstein's equation for a viscous fluid containing a dilute suspension of small, rigid, spherical particles.

$$\mu_{ef} = \mu_m (1 + 2.5\ \phi) \quad (6)$$

$$k_{ef} = k_m(1+7.4\ \phi)$$

Where, ϕ is the ratio of the volume of the nano-particle to the volume of the base fluid.

The symbols K_m and ϕ are the base fluid thermal conductivity and volume fraction of the nano-particle in the base fluid respectively.

The relevant thermo-physical properties of the solid nano-particles (Al_2O_3) used in the present study are Cp_p =773 J/kg.°C, ρ =3880 kg/m³, and k_p =36 W/m.°C, which are mentioned in previous work [10].

One can calculate the reduction factor in total thermal resistance of heat pipe charged with nanofluid by referring its thermal resistance to that charged with pure water, expressed as;

$$RR = (R_{water} - R_n)/R_{water} \quad (7)$$

The maximum relative error in total thermal resistance is about + 11.9 %.

4. Result and Discussion

Experiments are performed on heat pipe considering two different working fluids; pure water and Al_2O_3-water based nanofluid. In both cases, the effect of heat input rate, Q , and filling ratio, FR on its performance are investigated. Moreover, in case of the nanofluid, the effect of varying volume fraction of the nano-particles in the base fluid, ϕ, on the thermal performance of this heat pipe is also predicted. The values of local surface temperatures along all sections of the heat pipe are measured ($0 \le X \le 120$ mm), where X is measured from the beginning of the evaporator section. The range $0.0 \le X \le 40$ mm represents the evaporator section, $40 < X \le 80$ mm represents the adiabatic section and $80<X\le120$ mm represents the condenser section.

Figure 3 and 4 illustrate the surface temperature along the heat pipe for two values of heat input rate (40 and 60 W) and same filling ratio, FR of 0.45. As expected, the surface temperature decreases with increasing the

distance from the evaporator section due to the heat exchange between the heat pipe surface and working fluid. It is clear that the surface temperature decreases with increase of nano-particle concentration, ϕ. As expected, the surface temperature decreases with increasing the distance from the evaporator along heat pipe.

Figure 5 illustrates the variation of the total thermal resistance of the heat pipe, R with the filling ratio for Al_2O_3-water based nanofluid (ϕ =0, 0.5% and 1.2 %) at heat input rate of 40 W. As shown in the figure, R decreases with the increase of the filling ratio up to a value of FR equals to 0.40, after which R starts to increase with the increase of FR due to increasing liquid inside evaporator. It can be also noticed that the thermal resistance, R is inversely proportional to concentration of nano- particles, ϕ.

Figure 6 shows the variation of the total thermal resistance of the heat pipe, R with volume fraction of nano-particle in the base fluid, ϕ at two different heat input rates, Q (40 and 60 W). Over the tested range of ϕ, while keeping the filling ratio of 0.45, the percentage enhancement in R reaches up to 62.60% at $\phi = 1.2\%$ compared to its value when using pure water.

The effect of adding nano-particles on the thermal performance of the heat pipe is more evident if the data is expressed as a plot of the reduction rate in total thermal resistance, RR versus ϕ, as shown in figure 7, i.e. the enhancement of thermal performance is increasing with the increase of nano-particles concentration, ϕ. The addition of nano-particles has illustrated that during nucleate boiling some nano-particles deposit on the heated surface to form a porous layer. This layer improves the wet ability of the surface considerably. The thermal conductivity of the working fluid is also preferably high in order to minimize the temperature gradient.

The obtained heat transfer data is correlated as the following relation:

$$R = 0.294\left[K_q^{-0.596}\ FR^{1.273}\ \mathrm{Pr}^{-0.0532}\right] \quad (8)$$

The error in calculated thermal resistance is predicted by the above suggested correlation is around ±5 %, as shown in Fig. 8.

4.1. Comparison with the available literature

Figure 9 shows a comparison between the present experimental results with those reported by Kang [2] in case of using pure water as a working fluid with FR equals to 0.5. It can be observed that the present experimental results for the used two working fluids have the same trend as those reported by Kang [2]. The difference between both results when using pure water may be attributed to the difference in heat pipe geometry and uncertainty in measurements.

Figure10 shows a comparison between the present experimental results of the total resistance, R using Al_2O_3-water based nanofluid of ϕ =0.5% to those reported by Lips and Lefèvre [6] who used a heat pipe charged with n-pentane nanofluid of ϕ = 0.5%. One can see that the thermal resistance of the heat pipe decreases with increasing filling ratio up to a value of FR = 0.45, where it starts to increase with increasing the filling ratio. It can be also observed that the present experimental results are, a little bit, higher than those reported by Lips et al [6], but they have the same trend. The discrepancies in both results may be due to the differences in dimensions of the tested heat pipes as well as due to the type of working fluids used.

5. Conclusions

Using heat pipes and based on the nanofluid literature, particularly those related to the optimum operating condition, the thermal performance enhancement of heat pipes charged with the nanofluids indicates the potential of the nanofluid use as substitute of conventional fluids. This finding makes the nanofluid more attractive as a cooling fluid for devices with high power intensity. A compact heat pipe is thermally tested with two different working fluids; pure water and Al_2O_3-water based the nanofluid. The thermal performance of this heat pipe is predicted under different operating conditions including heat input rate, filling ratio, and volume fraction of the nano-particle in water. From the obtained data and its discussion, the following conclusions may be drawn:

1- The optimum filling ratio of charged fluid in the tested heat pipe was about 0.45 to 0.50 for both pure water and

Al_2O_3-water based the nanofluid, respectively.

2- By increasing concentration of the nanofluid, the thermal performance of heat pipe can be decreased

It can be said that better ability to manage thermal properties of working fluid translates into greater energy transport, smaller and lighter thermal systems. This may be applied to cooling of super computers.

References

[1] T. Kaya, R. Pe´rez, C. Gregori and A.Torres, "Numerical simulation of transient operation of loop heat pipes", Applied Thermal Engineering, vol.28, 2008, pp.967-974.

[2] S. W. Kang, W. C. Wei, S. H. Tsai, and S. Y. Yang, "Experimental investigation of silver nanofluid on heat pipe thermal performance", Applied Thermal Engineering, vol.26, 2006, pp.2377–2382.

[3] V.G. Pastukhov, Y. F. Maidanik, C.V. Vershinin, and M.A. Korukov, "Miniature loop heat pipes for electronics cooling", Applied Thermal Engineering, vol.23, 2000, pp.1125-1135.

[4] Y. W. Chang, C. H. Cheng, J. C. Wang, and S. L. Chen," Heat pipe for cooling of electronic equipment" Energy Conversion and Management, 2008.

[5] H. Jouhara1, O. Martinet, and A.J. Robinson, "Experimental Study of Small Diameter Thermosyphons Charged with Water", FC-84, FC-77 & FC-3283- 5th European Thermal-Sciences Conference, The Netherlands, 2008.

[6] S. Lips, F. Lefèvre, and J. Bonjou, "Combined effects of the filling ratio and the vapour space thickness on the performance of a flat plate heat pipe", International Journal of Heat and Mass Transfer vol. 53, 2010, pp. 694–702.

[7] S. K. Das, U.S. Choi, W. Yu, and T. Pradeep, "Nanofluid Science and Technology", Wily-Interscience, 2007.

[8] Das, S. K., Putra, N., Thiesen, P., and Roetzel, W., "Temperature dependence of thermal conductivity enhancement for nanofluids", J. Heat Transfer vol.125, 2003, pp. 567-574.

[9] R.B. Mansour, N. Galanis, and C.T. Nguyen, " Effect of uncertainties in physical properties on forced convection heat transfer with nanofluids," Applied Thermal Engineering Vol. 27, 2007, pp. 240–249.

[10] S. Lee, S.U.S Choi, S. Li., and J.A. Eastman, "Measuring thermal conductivity of fluids containing oxide nanoparticles," J. Heat Transfer vol. 121, 1999, pp. 280-289.

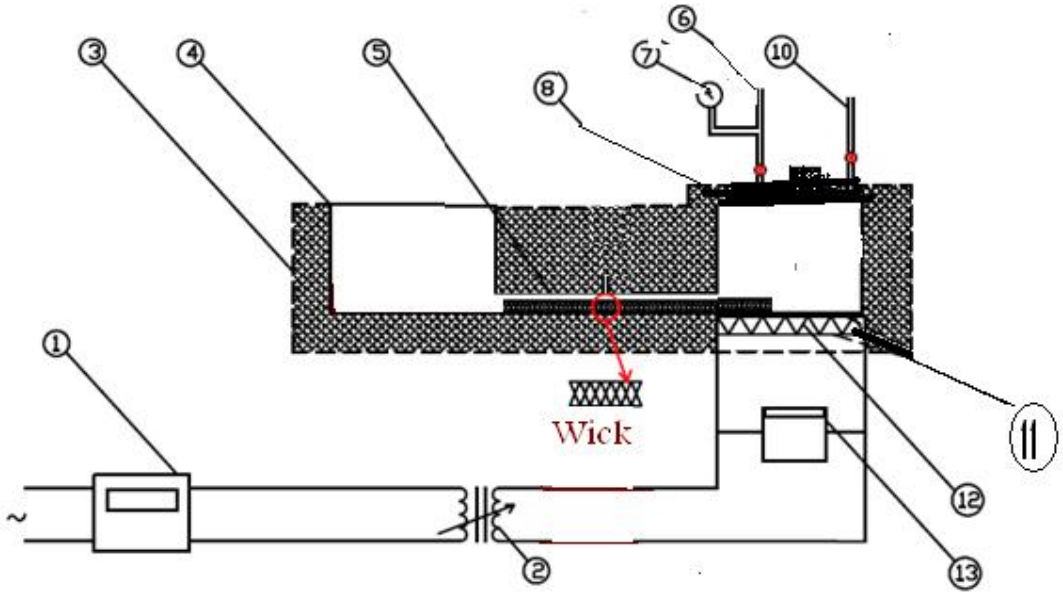

1. Stabilizer	2. Autotransformer	3. Insulation	4.condenser	5.Adiabatic tube
6. Charge line	7. Pressure gage	8. Evaporator		10. Vacuum line
11. Mica sheet	12. Electric heater	13. Multi-meter		

Figure 1 Schematic layout of the test rig

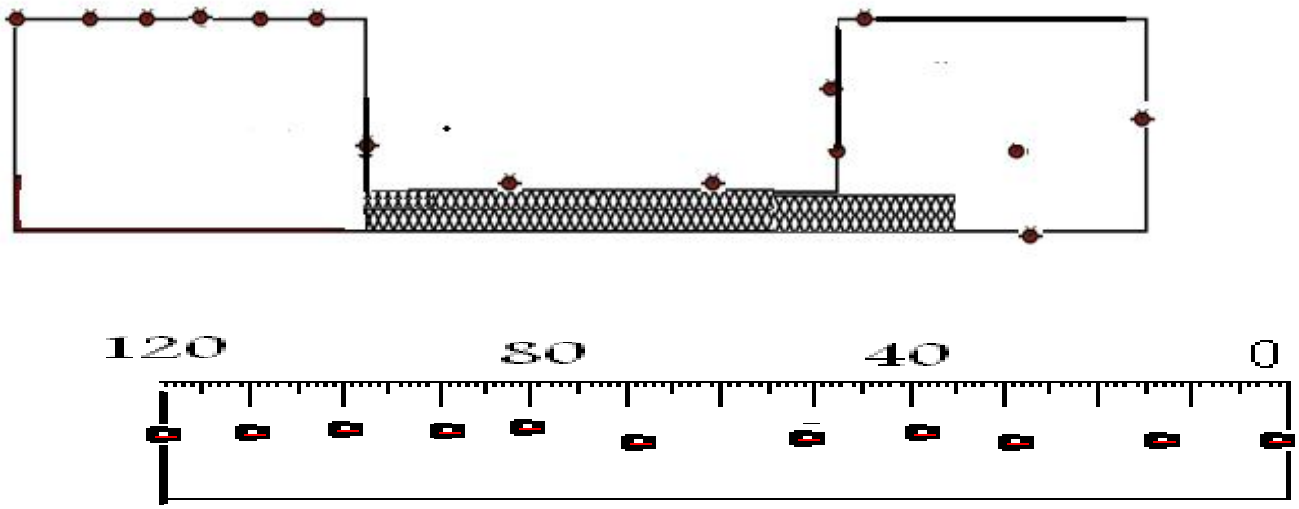

Figure 2 Thermocouples distribution along the heat pipe sections

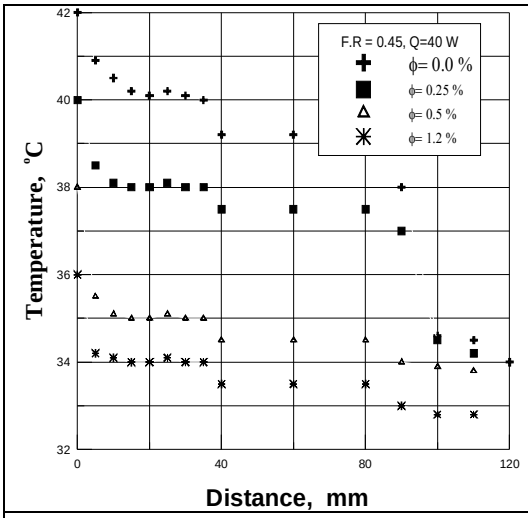

Figure 3 Temperature distribution along the heat pipe surface for different nanofluid concentration

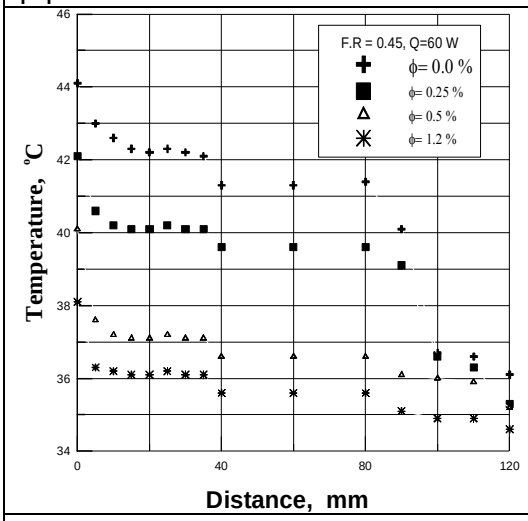

Figure 4 Temperature distribution along the heat pipe surface for different nanofluid concentration

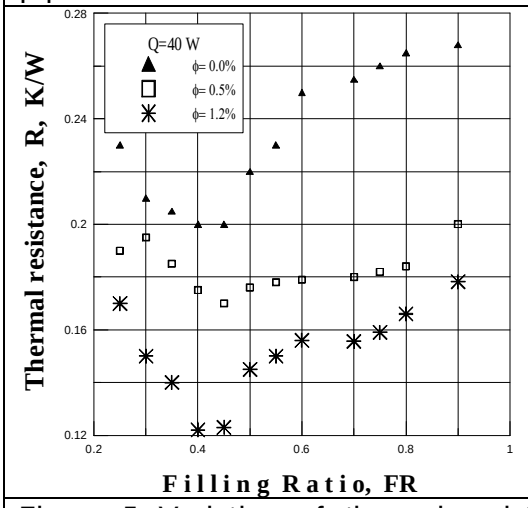

Figure 5 Variation of thermal resistance with filling ratio at different heat input rates

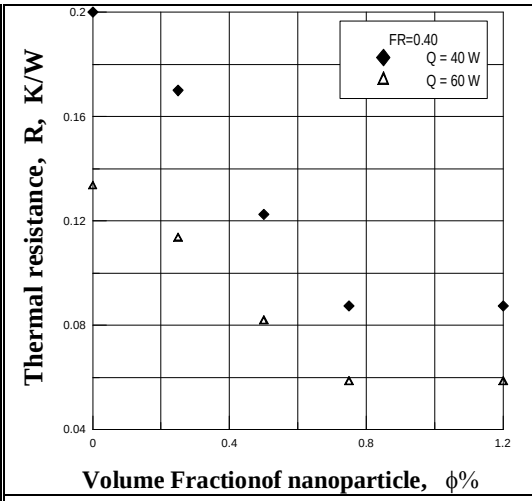

Figure 6 Variation of thermal resistance with volume fraction of nano-particles.

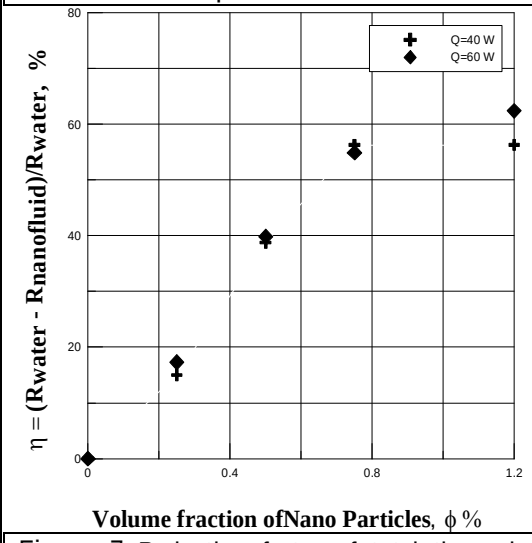

Figure 7 Reduction factor of total thermal resistance at different volume fraction of nano-particles, ϕ

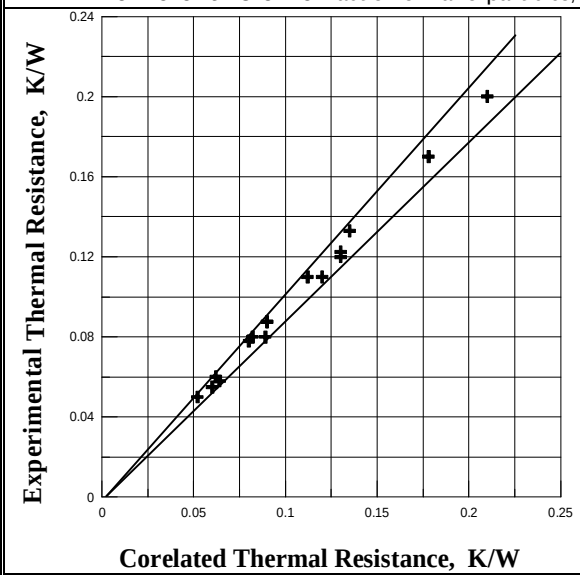

Figure 8 Experimental Nusselt number versus correlated

Nusselt number over the tested range of heat input rate

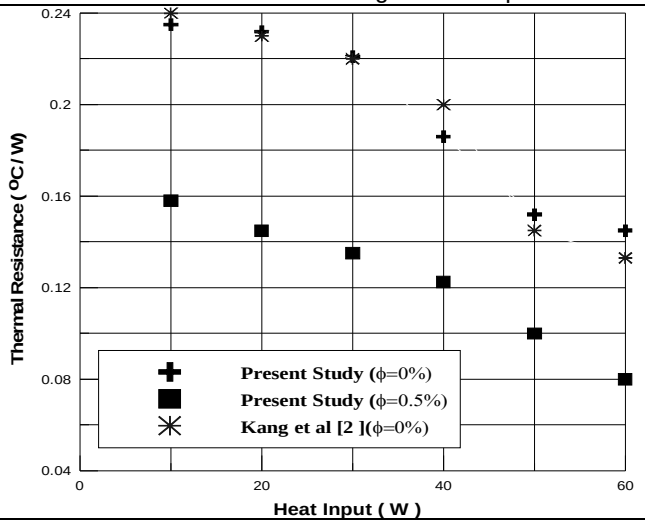

Figure 9 Comparison of the present results with available literature at different value of heat input rate

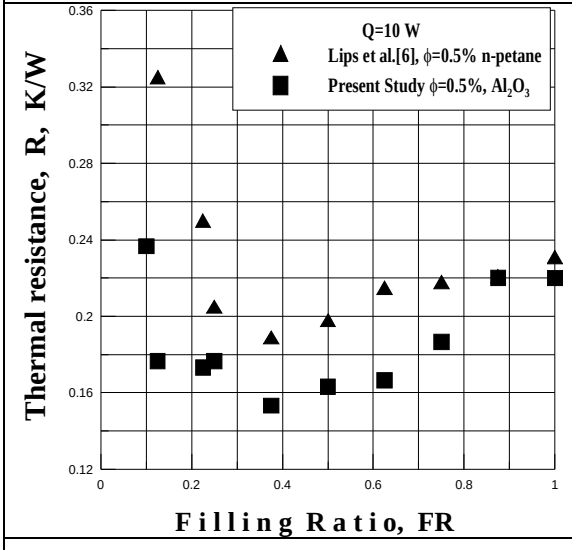

Figure 10 Comparison between present data and previous one for the variation of thermal resistance with filling ratio